

# Nonlinear control of the air feed of a fuel cell

Jorn K. Gruber and Carlos Bordons and Fernando Dorado

**Abstract**—This document presents the design of a hierarchical control to regulate the oxygen excess ratio of a fuel cell. The master controller calculates the necessary air flow to stabilize the oxygen excess ratio at a fixed set point. A nonlinear model based predictive controller (NMPC) using a Volterra series model is used as a master controller. The slave controller, a nonlinear PI, uses the reference of the air flow calculated by the master controller to stabilize the air flow in the compressor and allows reference tracking. The proposed control strategy is applied to full nonlinear model of a fuel cell in which simulations are carried out.

## I. INTRODUCTION

Fuel cells represent today the most efficient and clean way to convert energy chemically stored in fuel to electric energy. Furthermore, fuel cells provide the possibility of decentralized energy generation and allow mobile applications [1]. As a result of the continuously increasing demand for electric energy and emission regulations, the interest in fuel cells has augmented considerably. Of special interest are the fuel cells using a Proton Exchange Membrane (PEM) due to their high power density and the low operating temperature in comparison with other types of fuel cells [2].

For an efficient use of fuel cells it is necessary to control the air and hydrogen feed, the flow volumes and pressures as well as the water produced by the chemical reaction. During transitions the feed of the fuel cell has to be controlled to maintain temperatures, hydration of the membrane and partial pressures of the reactants in a suitable level to avoid membrane degradation and to maintain system's efficiency.

The principal control purpose of this work is to stabilize the oxygen excess ratio. Therefore the control acts over the oxygen inflow in order to supply an adequate amount of oxygen to the chemical reaction in the fuel cell stack. The reaction has to supply the electric current requested to the fuel cell by external consumers. Numerous control strategies have been proposed in order to approach the mentioned problem, containing dynamic feed-forward [3], LQR (linear quadratic regulator) [3] neural networks [4], robust control [5] and predictive control [6]. Various control configurations to regulate the oxygen excess ratio are presented in [7].

This document presents the design of a hierarchical control to regulate the oxygen excess ratio of a fuel cell. A nonlinear predictive controller based on a Volterra series model is

This research work is financially supported by the Spanish Ministry of Education and Science under the grant DPI2005-04568 and by MCYT-Spain under grant DPI2007-66718-C04-01.

The authors are with the Dept. de Ingeniería de Sistemas y Automática, Escuela Superior de Ingenieros, University of Seville, Spain jgruber@cartuja.us.es, bordons@esi.us.es, fdorado@cartuja.us.es

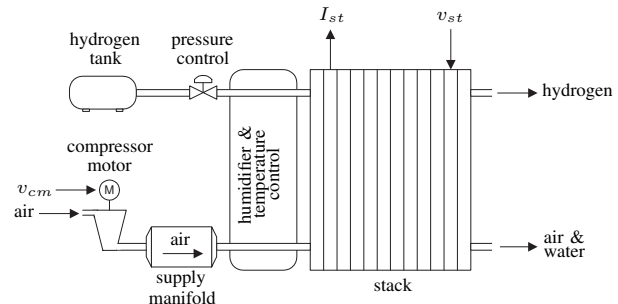
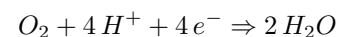


Fig. 1. General scheme of the fuel cell containing the stack and the auxiliary components.

used as a master controller. The master controller calculates the necessary air flow in the compressor which is used as a reference for the slave controller. The slave controller consists of a nonlinear PI allowing to track the reference calculated by the master controller. This work is arranged in the following way: the general functionality of a fuel cell and the nonlinear model used to carry out simulations are explained in section 2. In section 3 the design of the nonlinear PI and the predictive controller are shown. The designed control strategy is applied to the model of a fuel cell and its simulation results are shown in section 4. Finally, in section 5, the conclusions derived from the application of the designed control strategy are presented.

## II. FUEL CELL

The fuel cell model used in this document is a PEM fuel cell using hydrogen and oxygen from ambient air as fuel and oxidation medium, respectively. The hydrogen, stored in a tank, enters the stack on the anode side with a constant pressure. On the other side, the compressor aspirates environmental air and supplies it to the stack on the cathode side (see Fig. 1). The hydrogen reaching the catalyst anode is divided in protons and electrons of which the protons pass through the membrane towards the cathode. Due to the electric isolation of the membrane the electrons cannot pass through the membrane and are forced through an external circuit generating electric energy. In the cathode, the oxygen molecules, the electrons and the protons react and form water as a residual [3]:



One of the control objectives of fuel cells is the regulation of the oxygen excess ratio which is defined as follows:

$$\lambda_{O_2} = \frac{W_{O_2, supply}}{W_{O_2, reaction}}$$

TABLE I  
EQUATIONS OF THE NONLINEAR MODEL [8]

$$\begin{aligned}
 \dot{x}_1 &= c_1(-\chi + x_4) - \frac{c_3 x_1 \alpha(x_1, x_2)}{c_4 x_1 + c_5 x_2 + c_6} - c_7 w \\
 \dot{x}_2 &= c_8(-\chi + x_4) - \frac{c_3 x_2 \alpha(x_1, x_2)}{c_4 x_1 + c_5 x_2 + c_6} \\
 \dot{x}_3 &= -c_9 x_3 - \frac{c_{10}}{x_3} \left( \left( \frac{x_4}{c_{11}} \right)^{c_{12}} - 1 \right) h_{y_3}(x_3, x_4) + c_{13} u \\
 \dot{x}_4 &= c_{14} \left( 1 + c_{15} \left( \left( \frac{x_4}{c_{11}} \right)^{c_{12}} - 1 \right) \right) (h_{y_3}(x_3, x_4) - c_{16}(-\chi + x_4)) \\
 \chi &= x_1 + x_2 + c_2 \\
 \alpha &= \begin{cases} c_{17}(\chi) \frac{c_{11}}{\chi} c_{18} \sqrt{1 - \frac{c_{11}}{\chi} c_{12}}, & \text{if } \frac{c_{11}}{\chi} > c_{19} \\ c_{20}(\chi), & \text{if } \frac{c_{11}}{\chi} \leq c_{19} \end{cases} \\
 z_1 &= h_{y_1}(x_1, x_2)w - c_{21}u(u - c_{22}x_3) \\
 z_2 &= \frac{c_{23}(x_4 - \chi)}{c_{24}w} \\
 c_i &= cte. \forall i = 1, \dots, 24
 \end{aligned}$$

with  $W_{O_2, supply}$  denoting the oxygen supplied to the stack by the air flow and  $W_{O_2, reaction}$  representing the oxygen consumed by the chemical reaction. A value of  $\lambda_{O_2} < 1$  can physically harm the fuel cell as a consequence of starvation. Another control aim of fuel cells is to obtain a high net power. Both objectives can be reached regulating the air supply to the cathode. In the used model, the only control input is the voltage which allows the manipulation of the air flow through compressor and, as a consequence, the oxygen supply to the cathode. The stack current, depending on external consumers, has a big influence on the oxygen excess ratio and represents a measurable disturbance.

### A. Nonlinear model

The nonlinear model of the fuel cell used in this work is the 4 states nonlinear model presented in [8]. Temperature and humidity effects are not considered because of their slow dynamics in comparison with the dynamics of the air flow and the chemical reaction of oxygen. Besides, an ideal controller of the hydrogen pressure is assumed which allows a fuel supply with a constant pressure. The model equations can be seen in Table I and the constants are summarized in Table II. The physical parameters for the 75 kW fuel cell, used as a simulation model in this work, can be seen in the publications [8], [9].

The four states  $x = [x_1, x_2, x_3, x_4]$  represent the partial pressures of oxygen and nitrogen in the cathode channel, the angular velocity of the compressor and the air pressure in the supply manifold, respectively. The system input  $u = v_{cm}$  is the compressor motor voltage which allows the manipulation of the air feed and, as a consequence, the oxygen supplied to the fuel cell stack. The measurable disturbance  $w = I_{st}$  represents the current in the fuel cell stack. The system output  $y = [y_1, y_2, y_3, y_4]$  is the current in the stack  $y_1 = h_{y_1}$ , the air pressure in the supply manifold  $y_2 = x_4$ , the air flow in the compressor  $y_3 = h_{y_3}$  and the angular speed of the compressor motor  $y_4 = x_3$ , respectively. For further details on the functions  $h_{y_1}$  y  $h_{y_3}$  see the publications [1], [3].

TABLE II  
CONSTANTS OF THE FUEL CELL MODEL

$$\begin{aligned}
 c_1 &= \frac{RT_{st} k_{ca, in}}{M_{O_2} V_{ca}} \left( \frac{x_{O_2, atm}}{1 + w_{atm}} \right) & c_{13} &= \frac{\eta_{cm} k t}{J_{cp} R_{cm}} \\
 c_2 &= p_{sat} & c_{14} &= \frac{RT_{atm} k_{ca, in}}{M_{a, atm} V_{sm}} \\
 c_3 &= \frac{RT_{st}}{V_{ca}} & c_{15} &= \frac{1}{\eta_{ta} c_p} \\
 c_4 &= M_{O_2} & c_{16} &= k_{ca, in} \\
 c_5 &= M_{N_2} & c_{17} &= \frac{C_D A_T}{\sqrt{RT_{st}}} \sqrt{\frac{2\gamma}{\gamma-1}} \\
 c_6 &= M_v p_{sat} & c_{18} &= \frac{1}{\gamma} \\
 c_7 &= \frac{RT_{st} \eta}{4V_{ca} F} & c_{19} &= \left( \frac{2}{\gamma+1} \right)^{\frac{\gamma}{\gamma-1}} \\
 c_8 &= \frac{RT_{st} k_{ca, in}}{M_{N_2} V_{ca}} \left( \frac{1 - x_{O_2, atm}}{1 + w_{atm}} \right) & c_{21} &= \frac{1}{R_{cm}} \\
 c_9 &= \frac{\eta_{cm} k_i k_v}{J_{cp} R_{cm}} & c_{22} &= k_v \\
 c_{10} &= \frac{C_p T_{atm}}{J_{cp} \eta_{cp}} & c_{23} &= k_{ca, in} \frac{x_{O_2, atm}}{1 + w_{atm}} \\
 c_{11} &= p_{atm} & c_{24} &= \frac{n M_{O_2}}{4F} \\
 c_{20} &= \frac{C_D A_T}{\sqrt{RT_{st}}} \gamma^{\frac{1}{2}} \frac{2}{\gamma-1} \frac{\gamma+1}{2\gamma-2} & c_{12} &= \frac{\gamma-1}{\gamma} \\
 x_{O_2, atm} &= \frac{y_{O_2, atm} M_{O_2}}{y_{O_2, atm} M_{O_2} + (1 - y_{O_2, atm}) M_{N_2}} \\
 w_{atm} &= \frac{M_v}{y_{O_2, atm} M_{O_2} + (1 - y_{O_2, atm}) M_{N_2}} \frac{\phi_{atm} p_{sat}}{p_{atm} - \phi_{atm} p_{sat}}
 \end{aligned}$$

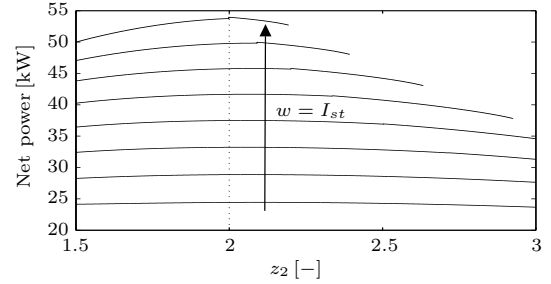


Fig. 2. Net power of the fuel cell in steady state for different oxygen excess ratios and currents in the stack.

Furthermore, the mathematical model uses the performance variable  $z = [z_1, z_2]$  with  $z_1$  as net power and  $z_2$  as oxygen excess ratio.

The control objective in this work is the stabilization of the oxygen excess ratio in a value of  $z_2^{ref} = 2$  in order to guarantee a high net power and to avoid a possible damage of the fuel cell as a result of starvation. As the net power reaches its maximum when the oxygen excess ratio is close to  $z_2 = 2$  (see Fig. 2) the proposed strategy does not control separately the net power.

### III. CONTROL DESIGN

This section presents the design of the hierarchical control strategy (master-slave) in which the master controller calculates the necessary reference for the air flow  $y_3^{ref}$  to obtain a oxygen excess ratio of  $z_2 = z_2^{ref} = 2$ . The slave controller manipulates the compressor motor voltage  $u = v_{cm}$  in order to obtain a compressor air flow of  $y_3 = y_3^{ref}$ . The slave controller, a nonlinear PI published in [10], guarantees global stability. As a master controller a nonlinear predictive controller based on a second order Volterra series model is taken in consideration. The hierarchical control strategy allows the use of a very fast slave controller which is not linked to the sampling time of the master controller. This

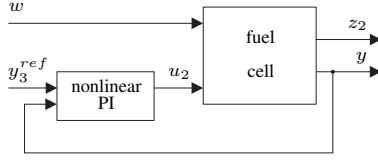


Fig. 3. Block diagram of the system consisting of the nonlinear PI controller and the fuel cell.

means that the slave controller could act several times in one sampling period of the master.

#### A. Slave controller – nonlinear PI

In first place, the slave controller that deals with the motor voltage  $v_{cm}$  in order to control the air flow  $y_3$  is designed. The air flow  $y_3(x_3, x_4)$  is strongly nonlinear [8] and depends on the supply manifold pressure ( $y_2 = x_4$ ) and the angular motor velocity ( $y_4 = x_3$ ). In order to guarantee stability and to consider the nonlinear character of the air flow, the nonlinear PI control presented in [10], has been chosen (see Fig. 3).

In order to apply this type of control, the derivative of the controlled output must have the following structure:

$$\dot{y} = \phi(y) + u \quad (1)$$

satisfying the condition  $0 \leq \phi(y) < 1$ . The control action and the integral part of the nonlinear PI control are defined as [10]:

$$\begin{aligned} u &= \beta(\beta_P(y) + \beta_I(y)) \\ \dot{\beta}_I &= w_I(y) \end{aligned} \quad (2)$$

In a first step, for the development of an adequate controller the desired system's dynamics  $\dot{y} = -\lambda y$  have to be chosen. Defining the signal

$$\chi = \beta_P(y) + \beta_I(y) \quad (3)$$

the system has the following dynamical behavior in closed loop:

$$\dot{y} = -\lambda y + (\phi(y) + \beta(\chi, y) + \lambda y) \quad (4)$$

With the close loop dynamics (4), it is necessary to find possible functions  $\beta_p$ ,  $w_I$  and  $\beta$  to guarantee the two conditions:

(I) for every  $y$  exists (at least) one solution  $\bar{\chi}_y$  for the algebraic equation

$$\phi(y) + \beta(\bar{\chi}_y, y) + \lambda y = 0$$

(II)  $\chi(t)$  converges asymptotically to  $\bar{\chi}_y$ .

A solution fulfilling conditions (I) and (II) and, as a consequence, guaranteeing global stabilization for  $\phi_m \leq \phi(y) \leq \phi_m$ , is presented in [10]. The proposed nonlinear PI has the form:

$$\beta = \dot{y}^{ref} - \lambda \tilde{y} - \phi_m - \frac{\phi_M - \phi_m}{1 + e^{-(\beta_P + \beta_I)/\tilde{y}}} \quad (5)$$

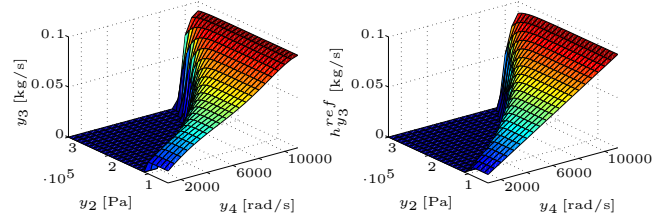


Fig. 4. Original (left) and approximated (right) function (7) of the compressor air flow.

with the tracking error  $\tilde{y} = y - y^{ref}$ . The proportional parameter  $\beta_P$  and the integral parameter  $\beta_I = w_I(y)$  are defined as [10]:

$$\beta_P = \frac{1}{2}y^2, \quad w_I(y) = \lambda y^2 \quad (6)$$

Using the definition of  $y_3 = h_{y_3}(x_3, x_4) = h_{y_3}(y_4, y_2)$  [1] it is impossible to express the derivative  $\dot{y}_3$  in the necessary form (1). For that reason the air flow  $h_{y_3}$  has been approximated with the following equation:

$$h_{y_3}^{apr} = \frac{y_3^{max} y_4}{y_4^{max}} \left( 1 - \exp\left(\frac{-r\left(s + \frac{y_4^2}{q} - y_2\right)}{s + \frac{y_4^2}{q} - y_2^{min}}\right) \right) \quad (7)$$

with  $r = 15$ ,  $q = 462.25 \text{ rad}^2/(\text{s}^2 \text{ Pa})$ ,  $y_4^{max} = 11500 \text{ rad/s}$ ,  $y_2^{min} = 50000 \text{ Pa}$ ,  $s = 100000 \text{ Pa}$  y  $y_3^{max} = 0.0975 \text{ kg/s}$ . Fig. 4 shows the original function and the approximation of the compressor air flow, respectively.

With the approximation (7) the derivative can be written as:

$$\dot{y}_3 = \phi(y) + m(y)u = \phi(y) + \nu$$

with  $0 \leq \phi(y) < \infty$  y  $m(y) > 0$ . This way, the derivative (8) allows the design of a nonlinear PI controller as described in [10]. In order to avoid chattering a new parameter  $\delta$  is included in the control law (5):

$$\nu = \dot{y}_3^{ref} - \lambda \tilde{y}_3 - \phi_m - \frac{\phi_M - \phi_m}{1 + e^{-(\beta_P + \beta_I)/(\tilde{y}_3 + \delta)}} \quad (8)$$

with

$$\delta = \begin{cases} \varepsilon & \text{if } \tilde{y}_3(t) > -\varepsilon, \exists t_0 < t \text{ s.t.} \\ & \tilde{y}_3(t_0) \leq -\varepsilon \text{ and } \tilde{y}_3(\tau) < \varepsilon, \forall \tau \in [t_0, t] \\ -\varepsilon & \text{if } \tilde{y}_3(t) \leq \varepsilon, \exists t_0 < t \text{ s.t.} \\ & \tilde{y}_3(t_0) \geq \varepsilon \text{ and } \tilde{y}_3(\tau) > -\varepsilon, \forall \tau \in [t_0, t] \end{cases}$$

and the regulation error tolerance  $\varepsilon > 0$ . Then, according to (8) and (8), the control action has the following form:

$$u = \frac{\nu}{m(y)} \quad (9)$$

#### B. Master controller – nonlinear MPC

In second place the master controller to calculate the reference for the nonlinear PI is designed. Fig. 5 shows the relation between the oxygen excess ratio  $\lambda$ , stack current  $I_{st}$  and compressor motor voltage  $v_{cm}$ . As can be seen, the oxygen excess ratio is strongly nonlinear for a low stack current. To consider the nonlinearity of the system and to allow an operation of the fuel cell over a wide range of

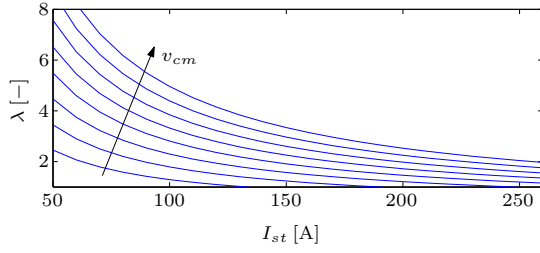


Fig. 5. Nonlinear relation between the oxygen excess ratio  $\lambda$ , stack current  $I_{st}$  and compressor motor voltage  $v_{cm}$ .

values for the stack current, a nonlinear predictive control based on a Volterra series model has been chosen.

As the used system is a stable fading memory system, it can be approximated by finite Volterra series models [11]. Defining the output  $y = \lambda$ , the input  $u = v_{cm}$  and the disturbance  $w = I_{st}$ , the truncated second order model can be expressed as follows:

$$y_k = h_0 + \sum_{i=1}^{N_{u_1}} a_{u,i} u_{k-i} + \sum_{i=1}^{N_{u_2}} \sum_{j=i}^{N_{u_2}} b_{u,ij} u_{k-i} u_{k-j} + \sum_{i=1}^{N_{w_1}} a_{w,i} w_{k-i} + \sum_{i=1}^{N_{w_2}} \sum_{j=i}^{N_{w_2}} b_{w,ij} w_{k-i} w_{k-j} \quad (10)$$

with  $h_0$ ,  $a_u$ ,  $b_u$ ,  $a_w$  and  $b_w$  denoting the offset, the lineal and second order parameters of the input and the disturbance, respectively. The parameters  $N_{u_1}$ ,  $N_{u_2}$ ,  $N_{w_1}$ ,  $N_{w_2}$  represent the truncation order for the corresponding parameters.

A very common input signal for linear model parameter identification is the pseudo random binary sequence (PRBS). In an analogous way, for the parameter identification of a nonlinear model a pseudo random multilevel sequence (PRMS) is used [12]. In order to collect suitable data, a PRMS was applied to the input of the system (fuel cell model + nonlinear PI). Furthermore, several changes in the disturbance were simulated. To obtain a wider range of data, values of  $w = I_{st} = \{100, 180, 260\}$  A for the disturbance were used. The values for the input  $u = v_{cm}$  are chosen in such a way that the resulting output  $y = \lambda$  lies in an interval of  $y = [1.3, 3]$ .

With the input–output data from the simulation, the parameter identification for nonlinear Volterra model was carried out by means of the least squares method. With a sampling time of  $t_m = 0.05$  s it was observed that the effect of a disturbance change is instantaneous. In contrast, after a modification of the input the system needs 40 sampling steps (2 seconds) to reach steady state. Finally, the model was identified with the truncation orders:  $N_{u,1} = 40$ ,  $N_{u,2} = 20$ ,  $N_{w,1} = 1$  and  $N_{w,2} = 1$ . The results of a second simulation were used to verify the identified model and to avoid a possible overparametrization. Both the results of the identification and the verification are shown in Fig. 6. The linear and second order parameters of the input are shown in Fig. 7.

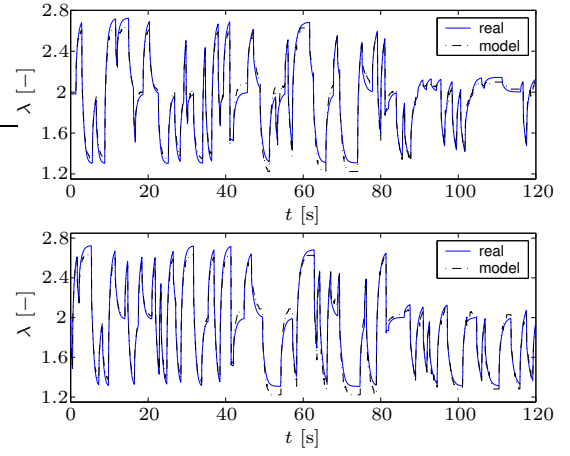


Fig. 6. Results of the identification (top) and verification of the identified model (bottom).

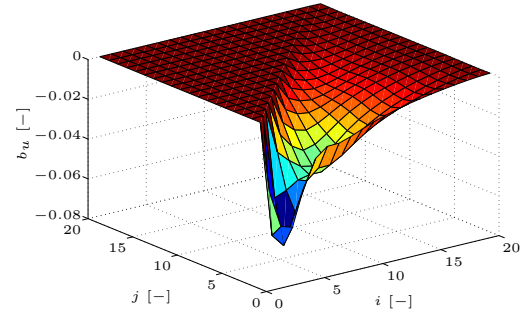
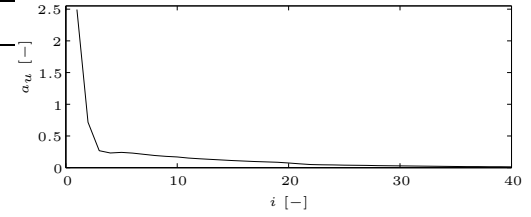


Fig. 7. Linear (top) and second order (bottom) parameters of the identified Volterra series model.

Finally, with the identified nonlinear model the control law for the NMPC is defined. The nonlinear model prediction in matrix form is defined as:

$$\mathbf{y} = \mathbf{G}_u \mathbf{u} + \mathbf{c} + \mathbf{f}_u \quad (11)$$

being  $\mathbf{y}$  the vector of predicted system output along the horizon used in the later described cost function (14). The terms  $\mathbf{G}_u \mathbf{u}$  and  $\mathbf{f}_u$  represent the linear and nonlinear part dependent on the future input, respectively. Note that the nonlinearity ( $\mathbf{f}_u$ ) is additive and therefore is included in the output as a new term. The vector

$$\mathbf{c} = \mathbf{H}_u \mathbf{u}_{pas} + \mathbf{g}_u + \mathbf{H}_w \mathbf{w}_{pas} + \mathbf{G}_w \mathbf{w} + \mathbf{g}_w + \mathbf{f}_w + \mathbf{d} \quad (12)$$

contains all the terms not depending on the current or future control actions. The matrices  $\mathbf{H}_u$  and  $\mathbf{H}_w$  denote the linear part of the past input and past disturbance, respectively. The matrix  $\mathbf{G}_w$  correspond to the linear part of the future disturbance values. The vectors  $\mathbf{u}$  and  $\mathbf{u}_{pas}$  contain the

future and past values of the control action and  $\mathbf{w}$  and  $\mathbf{w}_{pas}$  are the corresponding vectors for the disturbance. The future values of the disturbance are supposed to be constant, i.e.  $\mathbf{w} = [w(k), w(k), \dots, w(k), ]^T$ . The vector  $\mathbf{d} = [d(k), d(k), \dots, d(k), ]^T$  contains the difference between the process output and the estimated model output at instant  $k$ . The future–future and future–past terms of the input and the disturbance are represented by the vectors  $\mathbf{f}_u$  and  $\mathbf{f}_w$ , respectively. In analogous way,  $\mathbf{g}_u$  and  $\mathbf{g}_w$  contain the past–past terms of input and disturbance. A detailed description of the matrices  $\mathbf{G}_u$ ,  $\mathbf{H}_u$ ,  $\mathbf{G}_w$  and  $\mathbf{H}_w$  as well as how to calculate the vectors  $\mathbf{f}_u$ ,  $\mathbf{f}_w$ ,  $\mathbf{g}_u$  and  $\mathbf{g}_w$  can be found in Doyle *et al.* [14].

To consider the increments of the control action in the functional cost of the control law, (11) has to be transformed in a way that it depends on the increments of the control action  $\mathbf{y} = \mathbf{y}(\mathbf{u}) \rightarrow \mathbf{y} = \mathbf{y}(\Delta\mathbf{u})$ . Therefore, the following transformation using (11) and (12) has been made [13]:

$$\begin{aligned}
\mathbf{y} &= \mathbf{G}_u \mathbf{u} + \mathbf{c} + \mathbf{f}_u \\
&= \underbrace{\mathbf{G}_u \mathbf{L}}_{\mathbf{G}_u^*} \Delta\mathbf{u} + \underbrace{(\mathbf{H}_u + \mathbf{G}_u \mathbf{L} \mathbf{i})}_{\mathbf{H}_u^*} \mathbf{u}_{pas} + \mathbf{g}_u + \dots \\
&\quad \mathbf{H}_w \mathbf{w}_{pas} + \mathbf{G}_w \mathbf{w} + \mathbf{g}_w + \mathbf{f}_w + \mathbf{d} + \mathbf{f}_u \\
&= \mathbf{G}_u^* \Delta\mathbf{u} + \mathbf{f}_u + \dots \\
&\quad \underbrace{\mathbf{H}_u^* \mathbf{u}_{pas} + \mathbf{g}_u + \mathbf{H}_w \mathbf{w}_{pas} + \mathbf{G}_w \mathbf{w} + \mathbf{g}_w + \mathbf{f}_w + \mathbf{d}}_{\mathbf{c}^*} \\
&= \mathbf{G}_u^* \Delta\mathbf{u} + \mathbf{c}^* + \mathbf{f}_u \tag{13}
\end{aligned}$$

with  $\mathbf{L}$  being a lower triangular matrix and  $\mathbf{L} \mathbf{i}$  a matrix with ones in the first column and zeros in the other columns. For a detailed description of the transformation see [13].

Now, with the transformed nonlinear model, the cost function of the predictive control can include the increments in the control action

$$J = \sum_{i=1}^N (y(k+i) - r(k+i))^2 + \sum_{i=0}^{M-1} \theta \Delta u(k+i)^2 \tag{14}$$

where  $r(k)$  and  $\theta$  represent the output reference in instant  $k$  and the weighting function of the increments in the control action, respectively.

With the previous representation of the nonlinear model (13) and the cost function (14), an iterative approach to calculate the control action has been chosen. This approach, presented by Doyle *et al.* [14], represents an unconstrained NMPC. The scheme to calculate the control action is the following:

- Step 1: Set  $i = 1$
- Step 2: Solve the unconstrained least squares control problem

$$\mathbf{a} = \left( (\mathbf{r} - \mathbf{c}^* - \mathbf{f}_u)^T \mathbf{G}_u^* \right)^T \tag{15}$$

$$\Delta\mathbf{u} = (\mathbf{G}_u^{*T} \mathbf{G}_u^* + \lambda \mathbf{I})^{-1} \mathbf{a} \tag{16}$$

- Step 3: Verify if the first element of the calculated  $\Delta\mathbf{u}$  satisfies the desired tolerance  $\delta$  in condition

$$\left| \Delta u^{(i)}(k) - \Delta u^{(i-1)}(k) \right| < \delta \tag{17}$$

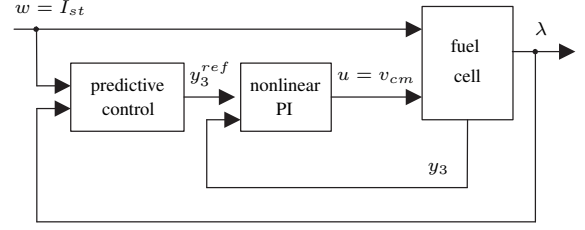


Fig. 8. Block diagram of the hierarchical controller consisting of a master controller (nonlinear predictive control) and a slave controller (nonlinear PI).

- Step 4: If the previous condition is satisfied, set  $\Delta u(k) = \Delta u^{(i)}(k)$  and calculate the new control action with  $u_p(k) = u_{pas}(k-1) + \Delta u(k)$  as

$$u(k) = \begin{cases} u_{min} & \text{if } u_p(k) < u_{min} \\ u_p(k) & \text{otherwise} \\ u_{max} & \text{if } u_p(k) > u_{max} \end{cases} \tag{18}$$

being  $u_{min}$  and  $u_{max}$  the lower and upper bound for the control action, respectively. If the previous condition is not satisfied, recalculate  $\mathbf{f}_u$  using

$$\mathbf{u} = u_{pas}(k-1) \cdot \mathbf{1} + \mathbf{L} \Delta\mathbf{u} \tag{19}$$

being  $\mathbf{1}$  a column vector with all entries equal to 1 and  $\mathbf{L}$  a lower triangular matrix. Set  $i = i + 1$  and return to step 2.

As can be seen in step 4, in case of failure to fulfill the convergence condition, in every iteration the future second order term  $\mathbf{f}_u$  is calculated with the vector of control actions  $\mathbf{u}$  calculated in the current iteration. During the iteration, the term  $\mathbf{f}_u$  is held constant and a new vector of control actions  $\mathbf{u}$  is calculated. This procedure is repeated until the difference between two vectors of control actions satisfies the convergence condition.

## IV. RESULTS

The control strategy presented was applied to the nonlinear model of the fuel cell (see Fig. 8). Several simulations were carried out in order to check the performance of the designed control scheme. Fig. 9 shows the simulation results with several steps in the disturbance. It can be seen that the applied control strategy compensates rapidly and with few oscillation the errors in the oxygen excess ratio. The nonlinear predictive controller shows a fast reaction and calculates a new reference for the compressor air flow. With the reference, the nonlinear PI computes finally the necessary system input  $v_{cm}$ . Furthermore the figure shows that the nonlinear predictive controller needs between 1 (steady state) and 12 (after a step in the disturbance) iterations to meet the convergence condition. The average computational time for the nonlinear control strategy (NMPC+ nonlinear PI) to resolve the optimization problem in one sampling instant is 14.7 ms, allowing the calculation of the control law within one sampling period (sampling time: 50 ms).

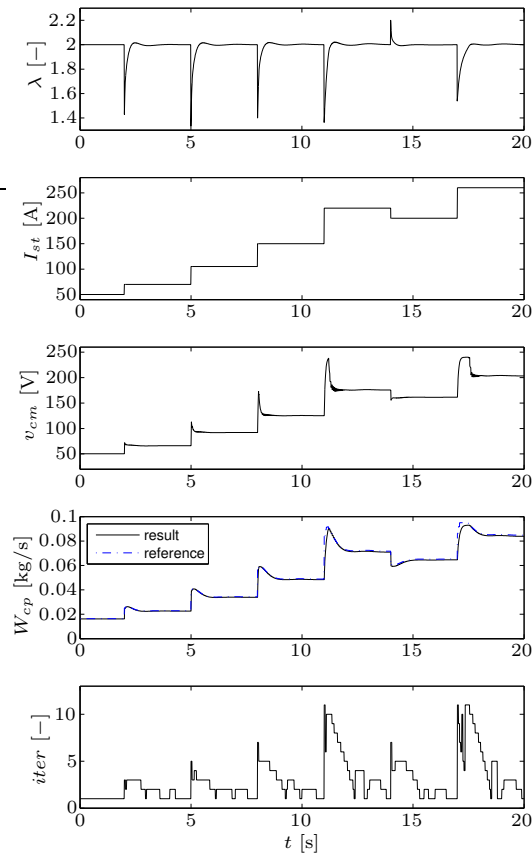


Fig. 9. Simulation results with step in the disturbance. From top to bottom: oxygen excess ratio, stack current, compressor motor voltage, compressor air flow and necessary iterations to solve optimization problem.

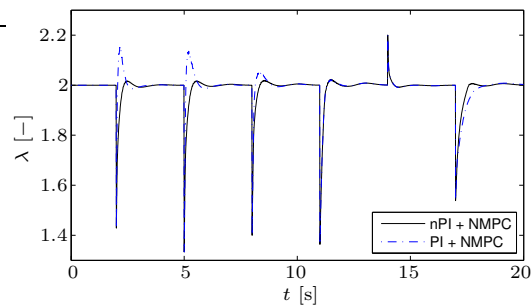


Fig. 10. Comparison of simulation results obtained with a linear and the nonlinear predictive control.

Fig. 10 shows a comparison between results of the NMPC + nonlinear PI and a control strategy with a NMPC + linear PI using the same disturbance trajectory as shown in Fig. 9. As can be seen, the combination of the NMPC with the nonlinear PI has a better behavior over a wide range of disturbance values. The linear PI in combination with the NMPC tends to oscillate for low disturbance values and to compensate errors slowly for high disturbance values.

## V. CONCLUSIONS

In this work the design of a hierarchical controller to control the oxygen excess ratio of a fuel cell has been

presented. The slave controller, a nonlinear PI, allows reference tracking of the compressor air flow. As a master controller a nonlinear predictive controller based on a second order Volterra series model was used. The master controller calculates the reference for the subordinated nonlinear PI with the objective to cancel the disturbance effects.

With the help of a nonlinear model of a fuel cell the behaviour of the hierarchical controller has been verified in simulations. The simulation results show that the hierarchical controller stabilizes the oxygen excess ratio in the desired value and reacts in a fast and efficient form to errors due to disturbances. The results have shown that the nonlinear PI is a good election to control strongly nonlinear systems and allows a fast reference tracking.

The comparison between the two control strategies (NMPC + nonlinear PI, NMPC + linear PI) showed that the strategy with the nonlinear PI stabilizes the oxygen excess ratio over a wide range of disturbance values presenting practically the same behaviour independently of the operation point.

## REFERENCES

- [1] M. Grujicic, K.M. Chittajallu, E.H. Law and J.T. Pukrushpan, "Model-based strategies in the dynamic interaction of air supply and fuel cell", *Proceedings of the 1 MECH E Part A Journal of Power and Energy*, vol. 218, no. 7, pp 487-499, 2004.
- [2] P.R. Pathapati, X. Xue and J. Tang, "A new dynamic model for predicting transient phenomena in a PEM fuel cell system", *Renewable Energy*, vol. 30, no. 1, pp 1-22, 2005.
- [3] J.T. Pukrushpan, A.G. Stefanopoulou and H. Peng, *Control of Fuel Cell Power Systems: Principles, Modeling and Analysis and Feedback Design*, Springer, London, 2004.
- [4] P.E.M. Almeida and M. Godoy Simoes, "Neural optimal control of PEM fuel cells with parametric CMAC networks", *IEEE Transactions on Industry Applications*, vol. 41, no. 1, pp 237-245, 2005.
- [5] F.C. Wang, Y.P. Yang, C.W. Huang, H.P. Chang and H.T. Chen, "Robust Control Design of a Proton Exchange Membrane Fuel-Cell System", *Proceedings of the European Control Conference 2007*, Kos, Greece, pp 978 - 983, 2007.
- [6] C. Bordons, A. Arce and A.J. del Real, "Constrained Predictive Control Strategies for PEM Fuel Cells", *Proceedings of the 2006 American Control Conference*, Minneapolis, Minnesota, pp 2486-2491, 2006.
- [7] J.T. Pukrushpan, A.G. Stefanopoulou and H. Peng, "Control of Fuel Cell Breathing", *IEEE Control Systems Magazine*, vol. 24, no. 2, pp 30-46, 2004.
- [8] K. Won Suh, *Modelling, Analysis and Control of Fuel Cell Power Systems*, Doctoral thesis, Department of Mechanical Engineering, University of Michigan, 2006.
- [9] J.T. Pukrushpan, H. Peng and A.G. Stefanopoulou, "Control-Oriented Modeling and Analysis for Automotive Fuel Cell Systems", *Journal of Dynamic Systems, Measurement and Control*, vol. 126, no. 1, pp 14-25, 2004.
- [10] R. Ortega, A. Astolfi and N.E. Barabanov, "Nonlinear PI control of uncertain systems: an alternative to parameter adaption", *Systems & Control Letters*, vol. 47, no. 3, pp 259-278, 2002.
- [11] S. Boyd L.O. and Chua, "Fading Memory and the Problem of Approximating Nonlinear Operators with Volterra Series", *IEEE Transactions on Circuits and Systems*, vol. CAS-32, no. 11, pp 1150-1161, 1985.
- [12] R.D. Nowak and B.D. Van Veen, "Random and Pseudorandom Inputs for Volterra Filter Identification", *IEEE Transactions on Signal Processing*, vol. 42, no. 8, pp 2124-2135, 1994.
- [13] J.K. Gruber and C. Bordons, "Control Predictivo no Lineal Basado en Modelos de Volterra. Aplicación a una Planta Piloto", *Revista Iberoamericana de Automática e Informática Industrial (in spanish)*, vol. 4, no. 3, pp 34-45, 2007.
- [14] F.J. Doyle, R.K. Pearson and B.A. Ogunnaike, *Identification and Control Using Volterra Models*, Springer, London, 2002.